

On the Suppression of Numerical Oscillations Using a Non-Linear Filter

W. SHYY, M.-H. CHEN, R. MITTAL, AND H. S. UDAYKUMAR

Department of Aerospace Engineering, Mechanics and Engineering Science, University of Florida, Gainesville, Florida 32611

Received November, 21, 1990; revised July 24, 1991

The idea of using a non-linear filtering algorithm to eliminate numerically generated oscillations is investigated. A detailed study is conducted to follow the development of numerical oscillations and their interaction with the filter. A relaxation procedure is also proposed to enhance the effectiveness of the filter. Three model problems, a 2D steady state scalar convection-diffusion equation, a 1D unsteady gas dynamics flow with shock and a 1D linear wave equation, have been designed to test the performance of the filtering algorithm. The effectiveness of the filter is assessed for convection schemes of different dispersive and diffusive characteristics, demonstrating that it is effective in eliminating oscillations with short wavelength, but oscillations of longer wavelengths are virtually unaffected. It is concluded that a proper combination of non-linear filter and dispersive numerical scheme is a viable alternative to dissipative schemes in resolving flows with sharp gradients and discontinuities. © 1992 Academic Press, Inc.

1. INTRODUCTION

The accurate representation of sharp gradients caused by phenomena such as shock waves, contact discontinuities, and internal/boundary layers has long been a challenge for the computational fluid dynamicist [1, 2]. It is well known that conventional numerical techniques often create spurious oscillations in these regions which can render the solution physically meaningless. Various remedies have been proposed. For example, Gresho and Lee [3] argued that the appearance of these unwanted oscillations can serve, at the most basic level, to indicate the regions that need finer grid spacings to improve the solution quality. Furthermore, based on this information one can improve the solution using various adaptive grid techniques, including grid redistribution [4-6] as well as local refinement [7-9]. Spurious oscillations can also be controlled either by using schemes that are intrinsically dissipative, such as the first-order upwind scheme, or by explicitly adding artificial viscosity to the governing equations to damp out numerical oscillations [1, 2]. Such methods tend to smear gradients and cannot adequately represent the complicated flow field unless fine grid spacing is used to

resolve the characteristics of flow in these regions. In order to more accurately control the amount of numerical dissipation, various TVD type schemes have been developed to capture sharp gradients without oscillations [2].

From a different perspective, one may also choose to extract the "useful," i.e., physically realizable information from oscillatory solutions obtained using unsatisfactory numerical schemes that are excessively dispersive. The idea is to eliminate undesirable portions of the solution while retaining only the desired; i.e., physically realizable ones. To this end, Engquist *et al.* [10] have recently devised a nonlinear filtering algorithm designed to work as a post-processor in conjunction with standard numerical schemes. In our view, the idea of using the filter to suppress numerical oscillations has an important implication. The main reason that prevents many high order schemes from being useful for the simulation of the convection-dominated flow problems is the appearance of non-physical oscillations. If a remedy can be developed to eliminate these oscillations, new ground can be broken in enhancing our capability of resolving large gradients in the flow field.

The present study attempts to analyze some of the basic features of numerical oscillations and to examine the role a non-linear filter can play in improving the overall numerical accuracy. Since, depending on the type of numerical scheme used, the numerical solutions may contain oscillations of different wavelengths, effects of the filter on oscillations of different wavelengths need to be delineated. This aspect will first be investigated. Furthermore, a relaxation procedure is proposed that can extend the effectiveness of the filtering algorithm originally proposed in Ref. [10].

In order to study the performance of the filter with respect to different sources of oscillations, several problems have been devised, including steady state and time-dependent flows, as well as single scalar and a system of simultaneous nonlinear equations. First, a scalar convection-diffusion problem of boundary layer type is solved. We choose three frequently used convection schemes for flows of the elliptic type, viz. second-order central differencing, second-order

upwind differencing [11] and a quadratic upwind differencing method called QUICK [12] to assess the impact of the filter on their performance. Next, the one-dimensional Navier–Stokes equations for flows with shock are solved. The onset and development of the spurious oscillations is followed. The interaction between numerical instability and non-linear filtering for both problems is interpreted in the context of wavelength selection. Based on these observations, a relaxation procedure is developed. It is tested by studying several popular methods [13], such as MacCormack, Lax–Wendroff, Beam–Warming in the case of a 1D linear wave equation.

2. FILTERING ALGORITHM

(I) Basics

As pointed out in Ref. [10], for a filter to be effective it should have minimal effect on an already smooth solution and should enforce some criterion to guarantee no spurious oscillations near discontinuities. Furthermore, it should achieve the above objectives with minimal computing expense. We have chosen the most rudimentary filter algorithm from Ref. [10]. More sophisticated algorithms have also been proposed, but they appear to be not as robust. Moreover, for the present purpose of understanding the characteristics of numerical instability and its interaction with the filtering scheme, the one described in the following serves very well.

Let ϕ_j be the variable obtained after solution of the conservation equations after n time steps and at grid index j . The filtering algorithm proceeds by first scanning the value ϕ_j to correct for local maxima or minima. When a correction is added at a point, the algorithm ensures that the same correction is subtracted from a neighboring point to maintain conservation. The corrected neighbor is taken as the one with the greater difference from ϕ_j . Furthermore, correction should be made so that no value may pass its neighbors. Thereby, overcompensation and creation of new extrema is avoided.

Specifically, let the symbols δ_+ and δ_- denote the forward and backward difference respectively, i.e., $\delta_+ \phi_j = \phi_{j+1} - \phi_j$ and $\delta_- \phi_j = \phi_j - \phi_{j-1}$. The filter algorithm works according to the following procedure:

(i) If $(\delta_+ \phi_j)(\delta_- \phi_j) < 0$, then ϕ_j is a local extremum, and it will be adjusted.

(ii) ϕ_{j+1} or ϕ_{j-1} must be adjusted by the same amount as ϕ_j is corrected; one of larger difference from ϕ_j will be chosen to be adjusted. The extent of correction applied to ϕ_j is limited to the smaller of ε_+ and ε_- , where ε_+ is equal to 0.5 times the larger one between $\delta_+ \phi_j$ and $\delta_- \phi_j$, and ε_- is equal to the smaller of the two differences.

It is noted that different correction schemes can be

devised in step (ii) to adjust the solution profiles. A relaxation procedure has been developed to modify the original scheme given above. As will be demonstrated, the proposed relaxation procedure can further improve the effectiveness of the filtering algorithm adopted here. The variables we feed into the filter at each time or iterative step are all the dependent variables to be solved. For the gas dynamics problem, they are density ρ , mass flux ρu , and the energy term $e = (\rho/(\gamma - 1) + \rho u^2/2)$.

(II) Interaction of Wavelength and Filtering

Oscillations of different wavelengths develop with time, depending on the particular numerical scheme employed. As it is designed, the filtering algorithm performs a search for a local extremum at each point in the domain and effects a correction in conjunction with an adjacent point; i.e., if a maximum is detected at position j , the value at j is decreased and at $j+1$ or $j-1$ is increased. This would indicate that the maximum effectiveness of the filter would apply to an oscillation of wavelength 2Δ , where Δ is the grid spacing. In the following we address the question as to how effective the present filtering algorithm can be when applied to the oscillations of longer wavelengths.

In order to interpret and quantify the performance of the filter an energy content E is defined

$$E^n = \left[\sum_{j=1}^J (\phi_j^n - \Phi_j)^2 \right]^{1/2}, \quad (1)$$

where ϕ and Φ are, respectively, the numerical and exact solutions, and the superscript n designates the number of times the filtering procedure has been applied. The symbol J indicates the total number of grid points.

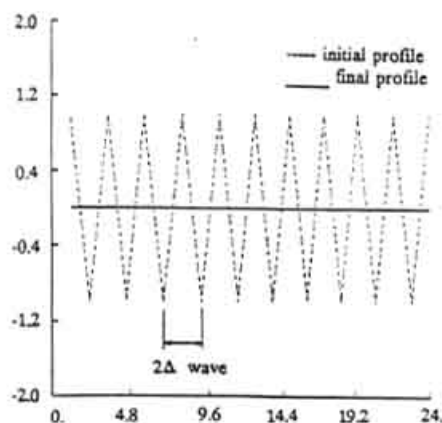


FIG. 1. Effect of filtering on oscillations with 2Δ wavelength. For this case one application is sufficient to suppress oscillation completely.

One can also define an area content, A , as follows:

$$A^n = \sum_{j=1}^J \phi_j^n. \quad (2)$$

According to the spirit of the present filtering algorithm, one attempts to minimize E^n while preserving A^n . In order to explore this issue, a series of test cases, each containing different wavelengths are designed. First, Fig. 1 demonstrates that a single application of the filter to a 2Δ oscillation is sufficient to eliminate all the oscillations. As one can clearly observe, after one application of the filtering algorithm, A remains the same and $E=0$, indicating that the goal has been achieved. If the same filter is applied to a 4Δ oscillation, it requires successive applications of the filter to suppress it. Figure 2 shows that the present filter proves to be very effective, with a geometric rate of reduction in E . In Fig. 2, E is normalized by the initial value, computed before applying the filter. Figures 1 and 2 collectively demonstrate

that there appears to be a clear wavelength dependence in terms of the effectiveness of the filtering algorithm. It turns out that the efficacy of the filter is restricted to oscillations of wavelengths no longer than 4Δ . To demonstrate this, Fig. 3 shows the performance of the filter with respect to long wavelength oscillations. Figure 3 compares the consequences of applying the nonlinear filter to three different oscillations with different wavelengths as well as waveforms. Figure 3a shows an oscillation initially of 6Δ wavelength and a triangular shape. After first application, the short wavelength portion, i.e., the tip of the oscillation is eliminated, reducing the normalized E^n to 0.633. Since a new plateau results from the filtering procedure, no further reduction of E^n is possible. Similarly, for a triangular wave of wavelength 8Δ , as shown in Fig. 3b, only the short wavelength components can be filtered out, with E staying at 95% of the initial value. Hence, the degree that the energy content E can be reduced decays very fast as the wavelength of the oscillation increases. Finally, Fig. 3c shows a sine-

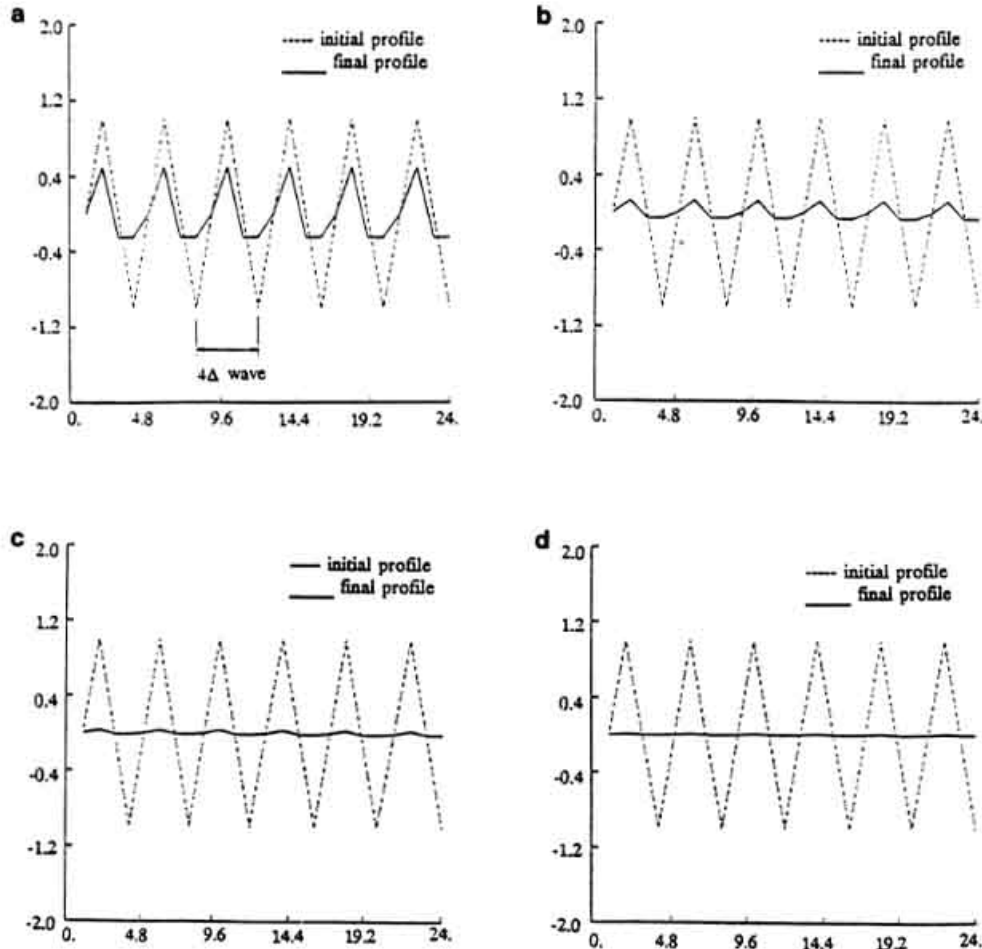


FIG. 2. Effect of successive application of filter on 4Δ oscillation: (a) First application, $E = 0.433$; (b) Second application, $E = 0.108$; (c) Third application, $E = 0.027$; (d) Fourth application, $E = 0.0067$.

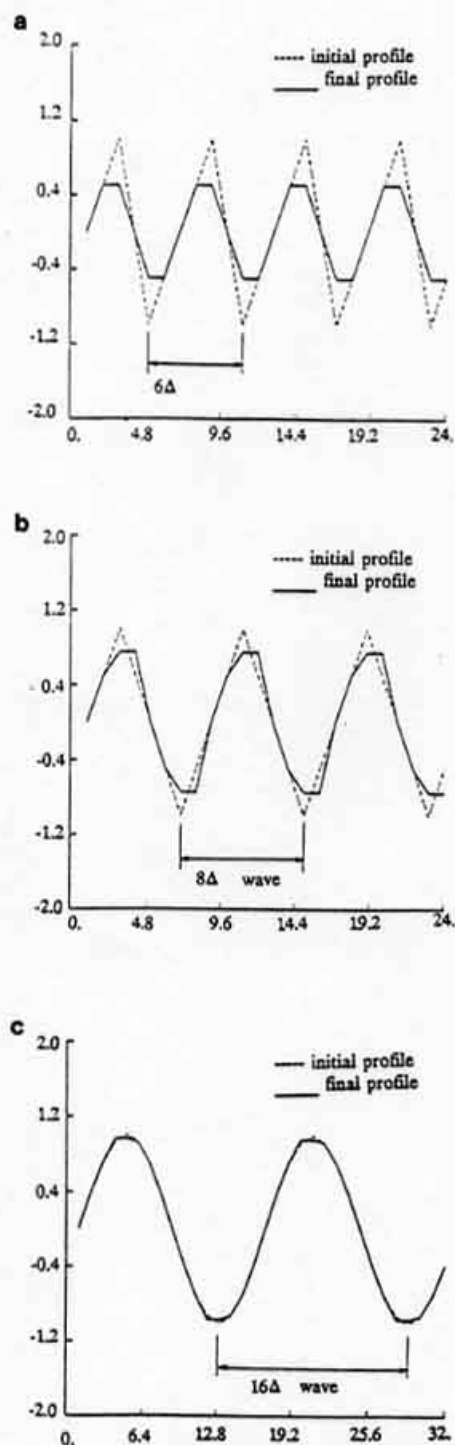


FIG. 3. Effect of filtering on oscillations with long wavelength. For these cases, the filter can only eliminate the short wavelength components: (a) 6Δ oscillation is not fully damped by filter after first filtering. Further application has no effect. $E = 0.633$; (b) 8Δ oscillation is not fully damped after first filtering. Further application has no effect. $E = 0.9574$; (c) 16Δ sine wave is only slightly altered after first filtering. Further application has no effect. $E = 0.999$.

wave of wavelength 16Δ , which is almost completely unaffected by the filter.

The inability of the filter to handle oscillations of long wavelengths may be an asset. For example, while solving an unsteady problem, with an appropriate numerical scheme, the present nonlinear filter can effectively eliminate short wavelength oscillations caused by the numerical procedure while only marginally affecting physically expected longer wavelength components. Hence it is not necessarily desirable to eliminate all the internal extrema present. However, in order to be able to distinguish between numerical oscillations and physical unsteadiness, the internal extrema caused by the numerics and physics must be separable. This means that in order to apply the filtering technique effectively, one would actually prefer to use a highly dispersive scheme such as the standard second-order central difference scheme that creates short wavelength oscillations. This is indeed the case as will be demonstrated later.

3. TEST PROBLEMS

In this section, test problems are used to demonstrate the characteristics of the numerical oscillations caused by various numerical schemes, and their interaction with the filtering technique. Three different problems with different solution characteristics have been chosen which include a single scalar 2D convection-diffusion equation for flow with a boundary layer, a complete set of 1D Navier-Stokes equations for flow with shock, and a 1D linear wave equation. For each case, unless otherwise noted, the filtering step is applied at the end of each time or iteration step. For the 2D case, the filtering step is applied along both directions in a sequential manner; the choice of sequence is inconsequential. As will be discussed later, it is important to apply the filter this way, for, otherwise, the wavelengths of the error can grow and the effectiveness of the filter can be diminished.

(I) Two-Dimensional Flow; Scalar Equation

The following two-dimensional convection-diffusion equation is considered:

$$u \frac{\partial \phi}{\partial X} + v \frac{\partial \phi}{\partial y} = \nu \left(\frac{\partial^2 \phi}{\partial x^2} + \frac{\partial^2 \phi}{\partial y^2} \right), \quad 0 \leq x \leq 1, 0 \leq y \leq 1, \quad (3)$$

with the Dirichlet boundary conditions:

$$\begin{aligned} \phi(0, y) &= 100 \\ \phi(1, y) &= 0 \\ \phi(x, 0) &= 0 \\ \phi(x, 1) &= 100. \end{aligned} \quad (4)$$

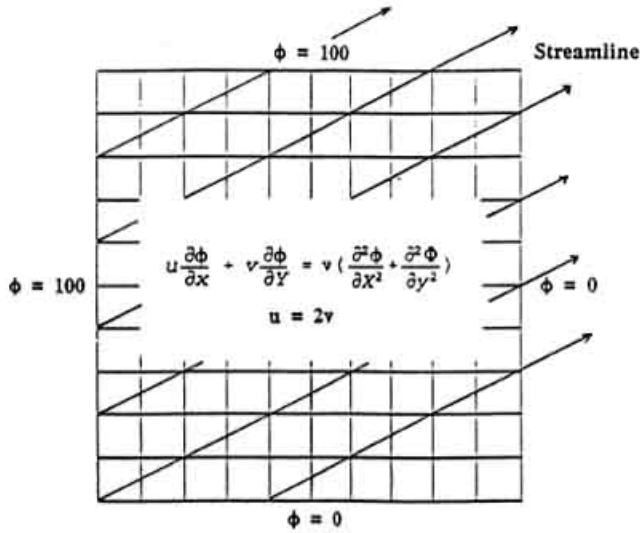


FIG. 4. Schematic of flow domain, boundary conditions, and grid system.

The geometry and boundary conditions adopted in the present study are shown in Fig. 4. The velocity components u and v are positive constants, with cell Peclet numbers, $Pe_{\Delta x} = u \Delta x / \nu = 10$. A 41×41 uniformly distributed grid system is employed. Due to the upstream and downstream boundary values assigned, a thin-layer type of solution exists near the downstream boundary. Three different convection schemes, namely, the second-order central difference scheme, the second-order upwind scheme, and QUICK have been adopted for comparison. The viscous terms are discretized according to the second-order central difference scheme for all cases. This model problem, along with the basic features of the schemes considered here have been investigated in Ref. [11].

The discretized form of the numerical schemes are:

(a) Second-order central difference scheme:

$$\begin{aligned} \phi_{i,j} = \frac{1}{4} & \left[\left(1 - \frac{Pe}{2} \right) \phi_{i+1,j} \right. \\ & + \left(1 + \frac{Pe}{2} \right) \phi_{i-1,j} + \left(1 - \frac{Pe}{4} \right) \phi_{i,j+1} \\ & \left. + \left(1 + \frac{Pe}{4} \right) \phi_{i,j-1} \right]; \end{aligned} \quad (5)$$

(b) Second-order upwind scheme:

$$\begin{aligned} \phi_{i,j} = \frac{1}{\left(4 + \frac{9}{4} Pe \right)} & \left[\phi_{i+1,j} + (2Pe + 1) \phi_{i-1,j} \right. \\ & - \frac{Pe}{2} \phi_{i-2,j} + \phi_{i,j+1} \\ & \left. + (1 + Pe) \phi_{i,j-1} - \frac{Pe}{4} \phi_{i,j-2} \right]; \end{aligned} \quad (6)$$

(c) QUICK scheme:

$$\begin{aligned} \phi_{i,j} = \frac{1}{\left(4 + \frac{9}{16} Pe \right)} & \left[-\frac{Pe}{8} \phi_{i-2,j} \right. \\ & + \left(\frac{7}{8} Pe + 1 \right) \phi_{i-1,j} + \left(1 - \frac{3}{8} Pe \right) \phi_{i+1,j} \\ & - \frac{Pe}{16} \phi_{i,j-2} + \left(\frac{7}{16} Pe + 1 \right) \phi_{i,j-1} \\ & \left. + \left(1 - \frac{3}{16} Pe \right) \phi_{i,j+1} \right]. \end{aligned} \quad (7)$$

The point SOR iterative method with under-relaxation is employed to obtain the steady-state solution for each

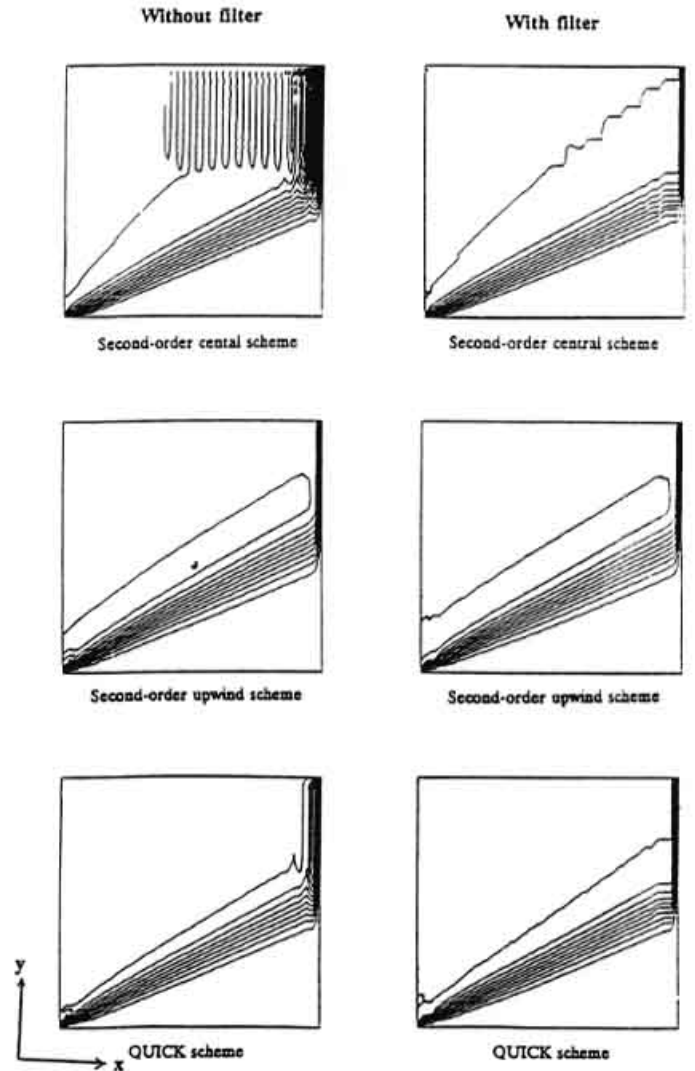


FIG. 5. Comparison of solution contours of 2D convection-diffusion scalar equation with and without filtering, on 41×41 uniform grid and cell Peclet number = 10.

scheme. A comparison of solution fields in the form of contour and profile plots of the three difference schemes with and without filters are depicted in Figs. 5 and 6, respectively. As already mentioned, a boundary-layer type solution is formed at the top right boundary. The fast variation of the variable ϕ across the boundary layer causes the second-order central difference scheme without filter to generate noticeable oscillations at the top boundary. The oscillations travel far into the upstream portion of the

domain. However, with the application of the filtering procedure at every iteration, the oscillations completely disappear, resulting in a more accurate and physically realizable solution.

It is noticeable that the filter exhibits different degrees of effectiveness on solution profiles at different locations. At $y = 0.875$, the solution with central difference scheme contains only the oscillations with 2Δ wavelength. The profile after filtering is of a constant value in the majority of the

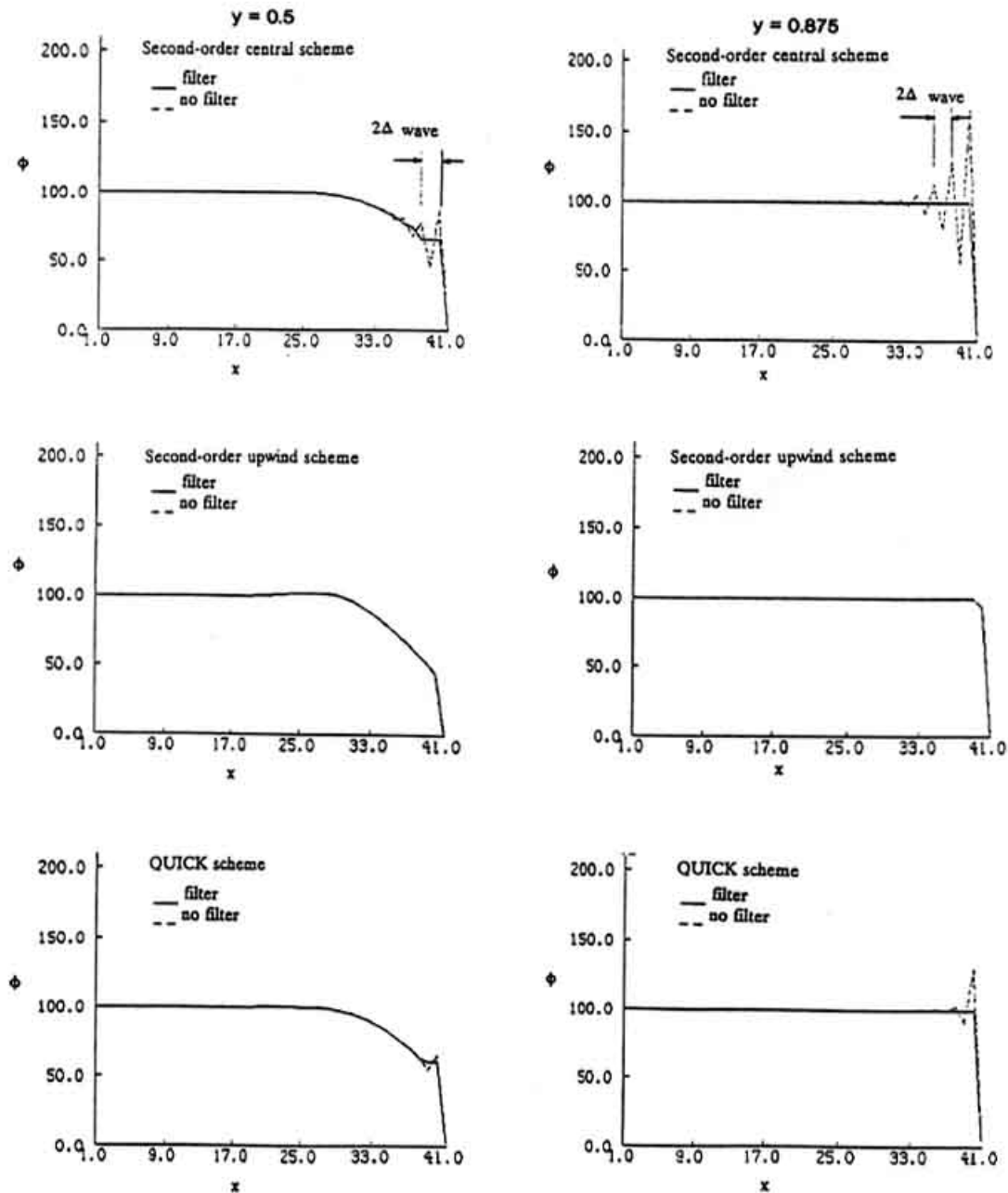


FIG. 6. Comparison of solution profiles of the 2D convection-diffusion scalar equation at two constant y -lines.

domain and exhibits a thin layer of the thickness of Δ , at the downstream boundary. Hence, according to our discussion in the previous section, the present filtering procedure can work very well there. However, the profile plot of a central differencing scheme with filter along the line of $y=0.5$ shows the "plateau" feature at the tail of the boundary layer. At $y=0.5$ the boundary layer is much thicker due to the cross-stream diffusion originating from the discontinuity of upstream boundary values. Hence, the numerical oscillations of wave length 2Δ , at $y=0.5$, ride on a smoothly varying profile whose characteristic length scale is much longer. Consequently, the filtering process creates several plateaus instead of a smooth curve for the final solution profile. In summary, the filter has the tendency of flattening extrema that are not the result of overshooting and thus gives a low order of accuracy locally around smooth extrema. This is a property shared with all TVD type schemes [14].

The second-order upwind scheme produces identical results with or without the filter; neither spurious oscillations nor noticeable plateaus are observed. This indicates that the filter is only active in regions of oscillations and does not much affect smooth solutions with no short wavelength oscillation. The numerical solution with the QUICK scheme without filter also exhibits oscillations near the boundary-layer region. Similar to the case of a central difference scheme with filter, the wiggles near the boundary-layer region are damped out, but the plateaus are still present.

From the results presented so far, several observations are readily made. First, the present filtering procedure is effective in eliminating 2Δ or 4Δ oscillations and ineffective for oscillations of longer wavelengths. Consequently it can improve the accuracy of the solutions yielded by both the central difference scheme and the QUICK scheme, transforming oscillations into smoother profiles with plateaus. With regard to the second-order upwind scheme, although the solution does exhibit a non-physical overshoot, because the overshoot is of a length scale larger than 2Δ , the filter in the present design cannot make any improvement. Consequently, without the filtering procedure the solution of the second-order upwind scheme is clearly better than those of other convection schemes. With the use of nonlinear filter, however, the solution of all three schemes are of comparable accuracy.

(II) One-Dimensional Flow with Shock

The problem just presented can clearly illustrate the salient features of the filtering algorithm. However, it is a linear equation containing a single scalar as a dependent variable. Next we investigate the performance of the filter in the context of a system of nonlinear equations with multiple dependent variables coupled together. Emphasis will be

placed on following the onset, growth, and subsequent development of numerical oscillations, and their interaction with the filter. As will become clear later, since for this nonlinear problem, the wavelength distribution of the oscillations widens as the computation proceeds, the timing of applying a filter is important.

A one-dimensional gas dynamics problem with a shock moving into quiescent gas is solved numerically.

The governing equations for the computations, in dimensionless form, are:

mass continuity,

$$\rho_t + (\rho u)_x = 0; \quad (8)$$

momentum,

$$(\rho u)_t + (\rho u^2 + p)_x = \frac{1}{\text{Re}_\infty} \left(\frac{\partial}{\partial x} \tau_{11} \right); \quad (9)$$

energy,

$$\begin{aligned} (\rho e)_t + [u(\rho e + p)]_x \\ = \frac{1}{\text{Re}_\infty} \left[\frac{1}{\text{Pr}_\infty} \frac{\partial}{\partial x} \left(\frac{\partial h}{\partial x} \right) + \frac{\partial}{\partial x} u \tau_{11} \right]; \end{aligned} \quad (10)$$

state,

$$p = \rho RT; \quad (11)$$

where

$$e = \left[\frac{(p/\rho)}{(\gamma-1)} + \frac{u^2}{2} \right] \quad (12)$$

$$h = \left(\frac{\gamma}{\gamma-1} \right) \left(\frac{p}{\rho} \right) \quad (13)$$

$$\tau_{11} = \frac{4}{3} \mu u_x. \quad (14)$$

Subscript ∞ in the above refers to values normalized with respect to free stream conditions.

The initial conditions are given as $P_2/P_1 = 1.5$; $\rho_2/\rho_1 = 1.22$; $P_2 = 10^5 \text{ N/m}^2$; $T_1 = 290 \text{ K}$, where subscripts 1 and 2 correspond to conditions downstream and upstream of the shock, respectively. These conditions correspond to an upstream Mach number of 0.28. The values of the Prandtl number, Pr , and the ratio of the specific heats, γ , are respectively 0.72 and 1.4. All calculations were made with $\Delta t/\Delta x = 0.03$, which was found to be within the stability limit.

An explicit time marching procedure based on the forward Euler method for time stepping is adopted. The equations are marched in time sequentially, from con-

tinuity, to momentum, and then to energy equation. A finite-volume approach is adopted to discretize the equations cast in the strong conservative law form. Two hundred uniformly distributed grid points are used. At the upstream boundary values of density, velocity, and pressure are specified, whereas, at the downstream boundary, pressure is specified and density and velocity are extrapolated from the interior points. In the above numerical scheme, the

dependent variables contained in the convection terms are treated by the first-order upwind scheme. The flux and pressure terms have been discretized by the second-order central difference schemes.

For subsonic flow behind the shock, since disturbances propagate along both upstream and downstream characteristics, central differencing of flux and pressure terms corresponds closely to the physics of the flow. On the other

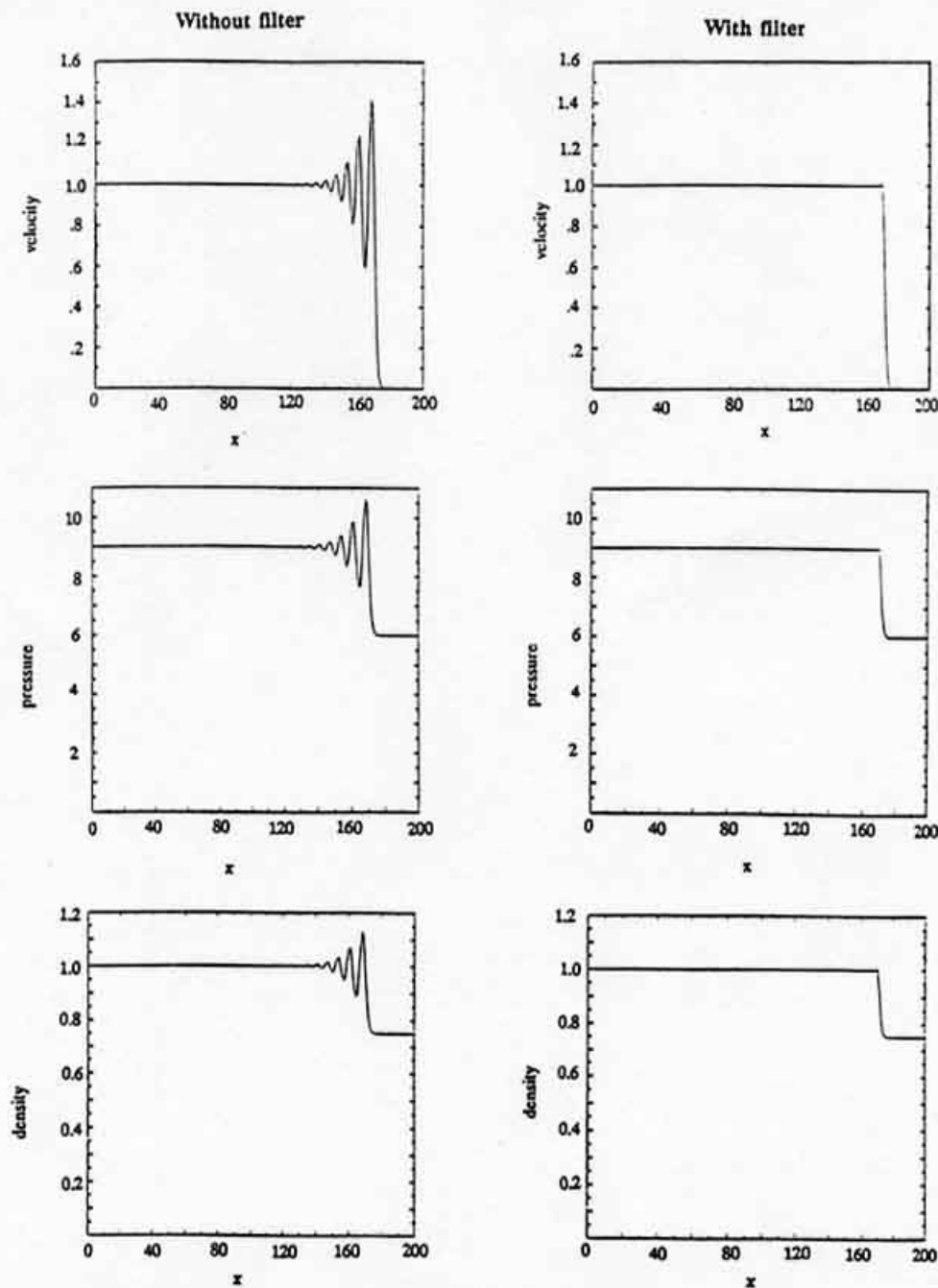


FIG. 7. Effect of filtering on a 1D compressible flow solution: $Re = 10^4$; time step = 600.

hand, using the first-order upwind scheme for the dependent variable is not consistent with the physics. It is well established that in order to correctly apply such an upwinding treatment of the convection terms, a flux-splitting [15] procedure based on the sign of the local eigenvalues is more appropriate. However, this practice is not adopted here for two reasons. First, it is known that flux-vector splitting along with the first-order upwind treatment is highly dif-

fusiveness and smears out sharp gradients resulting in a low level of accuracy. Second, for the present purpose, it is in fact our intention to generate spurious oscillations and then to investigate the effectiveness of the filtering algorithm. As will be demonstrated, it turns out that with the filtering procedure a very satisfactory solution results from an otherwise oscillatory one; furthermore, the final solution is more sharply resolved than could be obtained by the first order

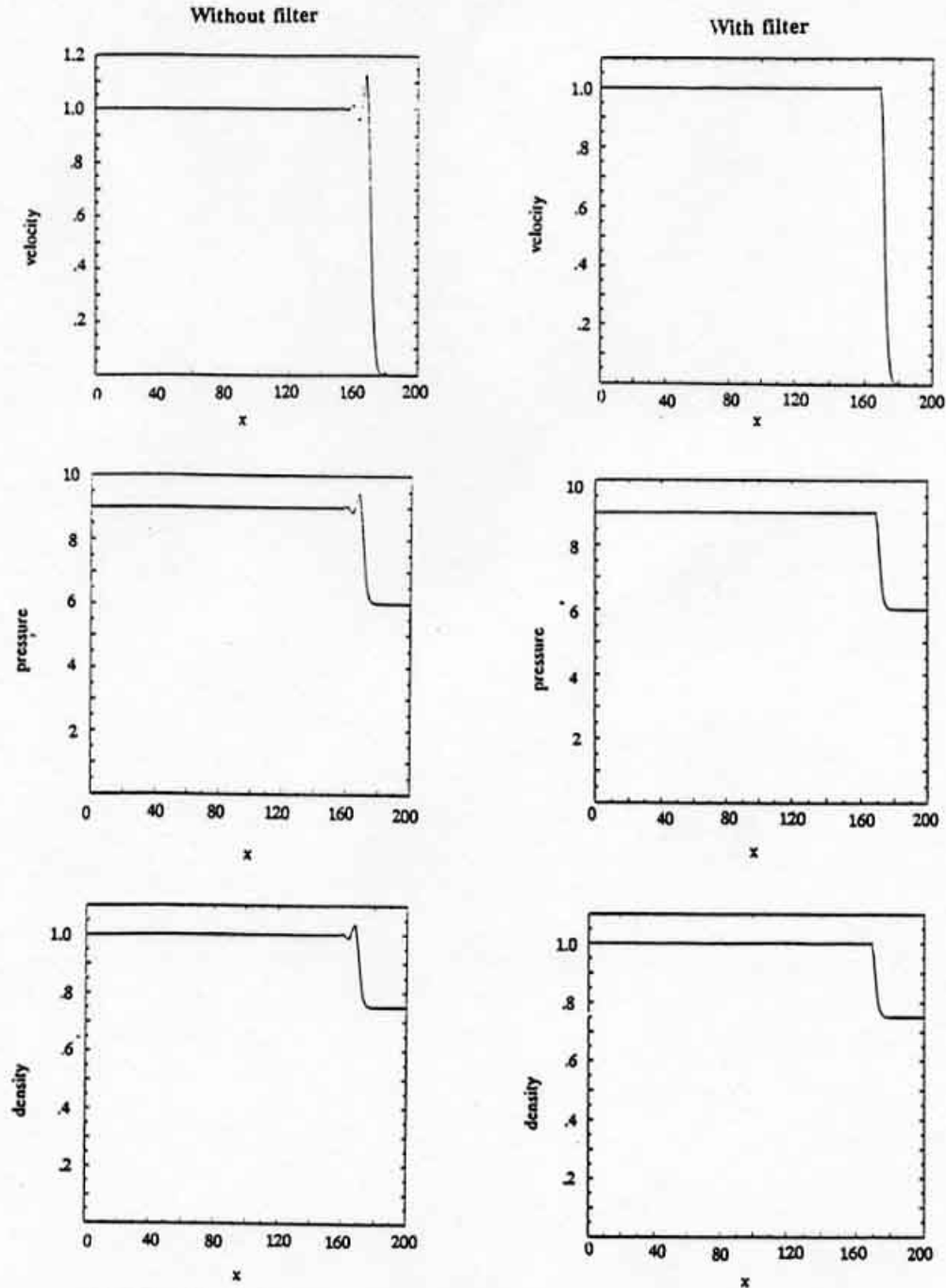


FIG. 8. Effect of filtering on a 1D compressible flow solution: $Re = 500$; time step = 600.

upwind scheme with flux-vector splitting, indicating that indeed it may be advantageous to utilize a filtering algorithm.

Two flow problems are considered with Reynolds number of 500 and 10^4 . For $Re = 10^4$, as shown in Fig. 7, solutions without filtering exhibit large oscillations propagating well into the upstream domain. When the filter is applied, sharp shock profiles are recovered without any evidence of oscillations. Figure 8 compares the solution with and without filter for a lower Reynolds number of 500. Without resorting to the filter, the solution is better behaved than for $Re = 10^4$. Nevertheless, in spite of a much larger viscous effect for $Re = 500$, oscillations still exist near the discontinuity. When the filter is applied, the oscillations disappear and a satisfactory solution is obtained. Figures 7 and 8 demonstrate that the filtering technique works extremely well for the present problems. The resulting solutions are not only oscillation free, the shock is sharper than commonly yielded by a first-order scheme.

In the previous section, we have discussed and demonstrated the wavelength selection characteristic intrinsic to the present filtering algorithm. However, both Figs. 7 and 8 show that for solutions without a filtering procedure, the characteristic wavelength of the oscillations are longer than 2Δ or 4Δ ; they are around 10Δ in both cases. Hence the fact that the filtering procedure is effective clearly suggests that the onset of instability for the present numerical method must be of short wavelengths. These initial oscillations apparently grow in time, not only in magnitude but also in wavelength. In order to explore this aspect of instability formation and growth, a detailed scrutiny of the evolution of solution profile with time is conducted in the following.

Figure 9 shows a sequence of velocity profiles after selected time steps at locations upstream of the discontinuity. Up to 10 time steps, the numerical oscillations initially form with a 2Δ wavelength and grow in magnitude but not in wavelength. After 30 time steps, a bifurcation of wavelength appears and both 2Δ and 3Δ waves are observable. The situation remains qualitatively the same until after 100 time steps, when an additional wavelength of 4Δ appears. This scenario of growth and bifurcation continues until a steady profile as in Fig. 7 results. Figure 9 shows the solution profiles for $Re = 10^4$ without using the filtering procedure at three instants, viz. after 10, 30, and 100 time steps. Figure 10 shows the solution profiles after the filter has been applied only once to the corresponding situations in Fig. 9. In the cases of Figs. 7 and 8, the filter is invoked at every time step, whereas in Fig. 10 only one application has been made at the time step shown.

The results displayed in Fig. 10 again confirm our earlier analysis regarding the wavelength dependence of the filtering procedure. If the filter is applied after 10 time steps, then since all the oscillations are of 2Δ wavelength, the solu-

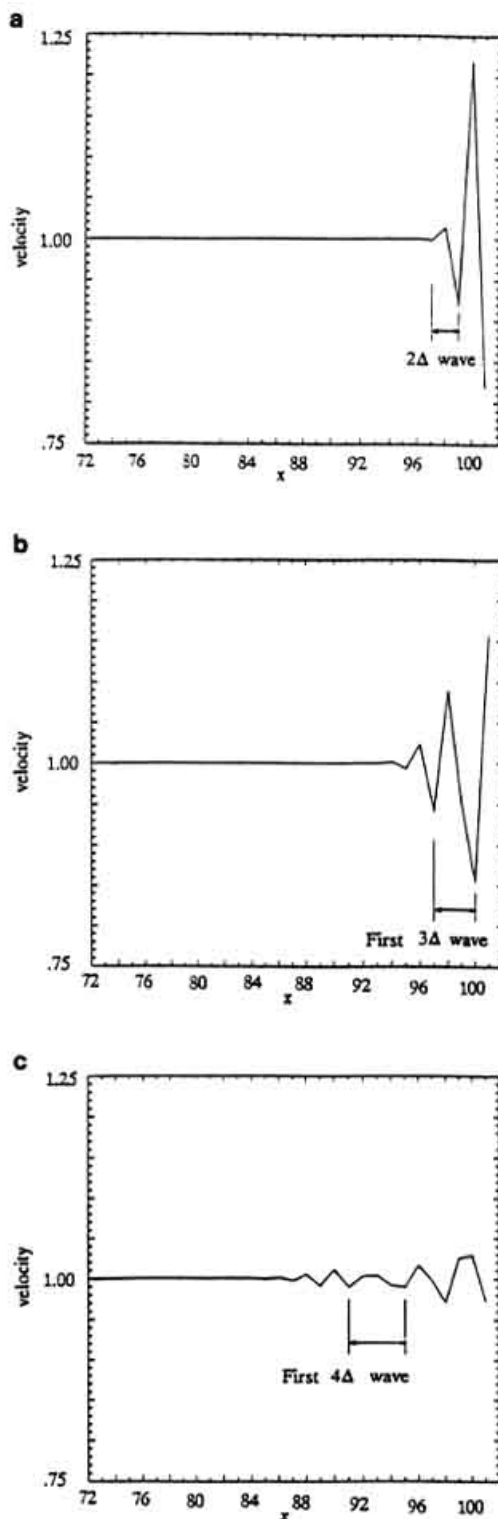


FIG. 9. Sequence of development of oscillations with time. Profile shown is of a segment upstream of the shock. The ordinate has been scaled to magnify the amplitude of the wave: (a) a typical 2Δ oscillation present at time step = 10; (b) first 3Δ oscillation appears at time step = 30; (c) first 4Δ oscillation appears at time step = 100.

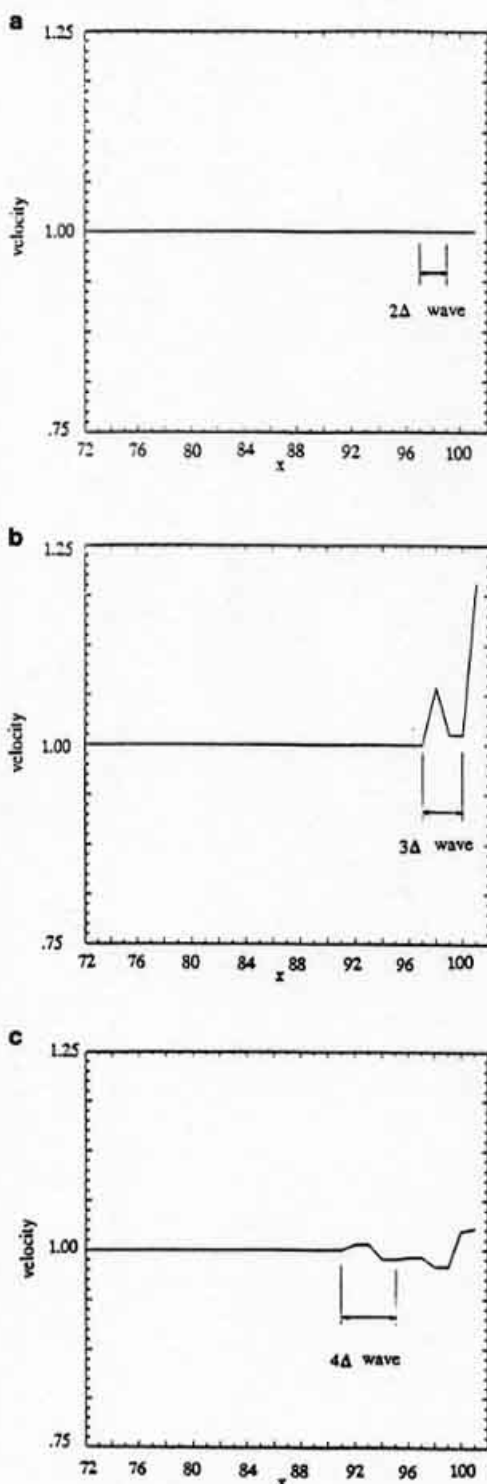


FIG. 10. Effect of filtering on oscillations. Here filter is applied once after the time step indicated. The figures show effect of one application of filter: (a) 2Δ oscillation is eliminated after one application; (b) Filter is not able to eliminate the 3Δ oscillation completely; (c) 4Δ oscillation is not eliminated and plateaus are formed after one application.

tion is immediately freed of any oscillations. If it is applied after 30 time steps, then as shown in Fig. 10, after one application of the filtering procedure, all 2Δ waves disappear and only the 3Δ wave remains. The 3Δ wave can be further suppressed after successive application of the filtering procedure. Finally, if the filter is applied only after every 100 time steps, as shown in Fig. 10, then after one application, all 2Δ waves again disappear while the longer ones remain. As the wavelengths become longer the filter effectiveness diminishes. If one waits until the steady state form shown in Fig. 7 is reached, since the characteristic wavelength of the oscillations is long, the filter is found to contribute very little to improve the solution accuracy.

(III) Filtering with Relaxation

The result presented so far are all based on the procedure outlined in Section 2(I). It should be noted that the filtering procedure does not yield unique solutions. Different procedures can be devised that can adjust the solution profiles differently; these different adjustment paths can result in different final solutions with different degrees of dispersion and dissipation characteristics.

In the course of this study, it has been found that step (ii) outlined in Section 2(I) can be modified by incorporating a relaxation procedure during the correction step; if the correction to be made is multiplied by a relaxation parameter ω , usually larger than 1, then the filtered solution can be further improved to satisfy its physical realizability. Essentially, the relaxation procedure incorporates extra adjustments by removing the plateaus, encountered in the early stage of filtering procedures, while still satisfying the idea of area preservation. In order to investigate the effectiveness of this relaxation procedure, the 1D linear wave equation with a constant speed of propagation is used as the model problem. It is noted that all the results presented in Figs. 5–8 have reached such levels that the present relaxation procedure does not alter them. However, the following examples show that there are many cases for which a relaxation procedure can further improve the quality of the solution.

The test problem devised here is the simple 1D linear wave equation,

$$\frac{\partial \phi}{\partial t} + u \frac{\partial \phi}{\partial x} = 0, \quad t > 0, \quad -\infty < x < \infty, \quad (15)$$

with a constant value of u , and a step function as the initial condition. Four common schemes are used to solve this problem with 101 grid points and the Courant–Friedrichs–Lewy (CFL) number of 0.5. The schemes tested are the standard Lax–Wendroff, Beam–Warming, MacCormack, and the combination of forward Euler (time)/second-order upwind (space). Detailed formulas can be readily found

from many standard references, e.g., [13], and will not be repeated here.

Figure 11 shows the solution obtained using these schemes after 50 time steps with three treatments, i.e., without application of a filter, those with the filtering procedure as outlined in Section 2 (or, in the present context, with $\omega = 1.0$), and filtering with a relaxation parameter with $\omega = 1.6$. As can be clearly observed, solutions without fil-

tering are all unsatisfactory, yielding oscillations of different magnitude and wavelengths. In particular, the combination of forward Euler/second-order upwind scheme does not seem to be able to produce a solution of any use at all. In this regard, it should be noted that other time-stepping schemes such as the second-order Runge-Kutta method, when combined with the second-order upwind scheme, can yield solutions with greatly reduced oscillations. We decided

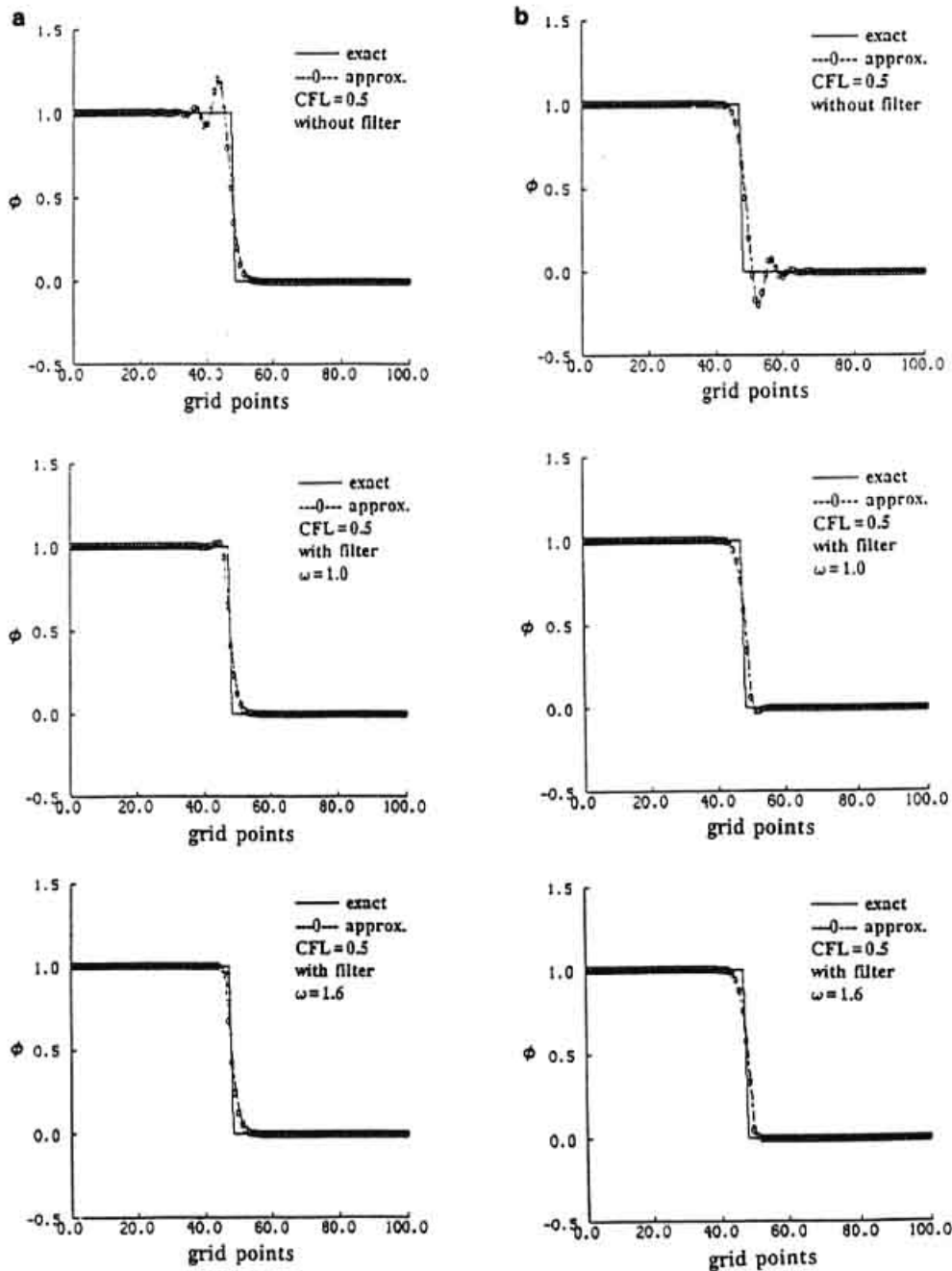


FIG. 11. Effect of relaxation parameter on the performance of filtering procedure, 1D linear wave equation: (a) MacCormack scheme; (b) Beam-Warming scheme; (c) Lax-Wendroff scheme; (d) forward Euler/2nd-order upwind.

to use this particular combination to contrast the effect of the filtering algorithm. With the use of the filtering algorithm and $\omega = 1.0$, it is clear that all the solutions are improved, exhibiting attenuation of spurious oscillations. Nevertheless, it is also clear that the filtering algorithm cannot completely suppress the wiggles and the internal plateaus that appear within each solution. This phenomenon is due to the fact that the schemes tested here all

contain some levels of built-in dissipation, and, hence, some oscillations with longer wavelengths are retained at the end of the filtering procedure. However, if $\omega = 1.6$ is used, instead of 1.0, the solution can be further improved and all the undesirable wiggles disappear. In fact, the final solutions of all the schemes are of high quality, maintaining sharp profiles across the discontinuity with no spurious oscillations. In particular, that resulting from the forward Euler/

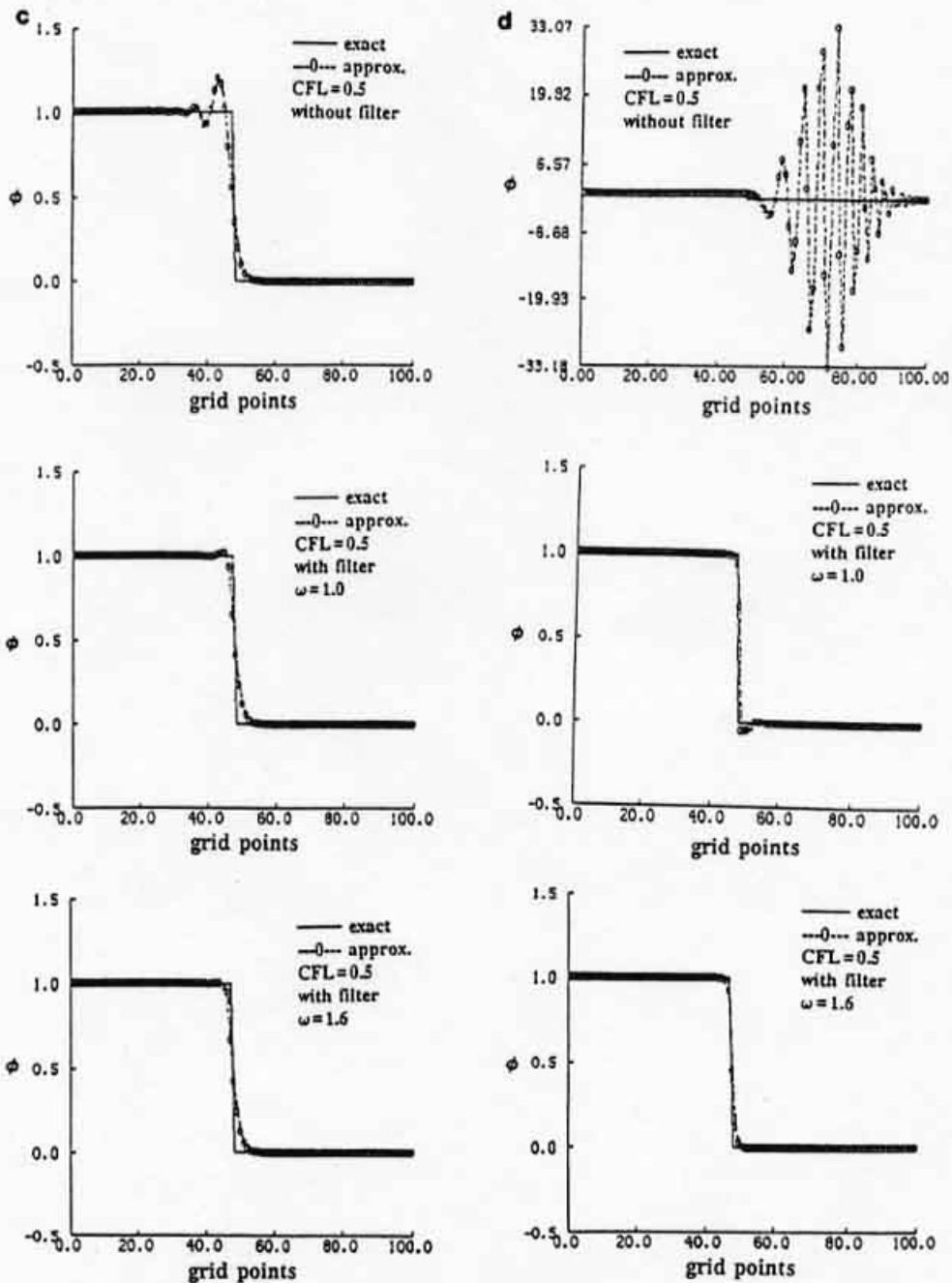


FIGURE 11—Continued

second-order upwind combination is of sharper gradient across the discontinuity than others. The results contained in Fig. 11 again demonstrate that when properly handled, the spurious components of a seemingly useless solution can actually yield very good quality, yielding satisfactory solutions from the viewpoint of physical realizability as well as quantitative accuracy.

4. CONCLUSIONS

The non-linear filter has proved to be very effective in suppressing numerically generated oscillations of 2Δ and 4Δ wavelengths. The fact that the filter primarily affects small wavelength oscillations proves to be a desirable feature. For any numerical simulation, grid independence studies can be used to delineate the spurious oscillations from the physical ones and a grid size chosen such that physical waves are of relatively longer wavelengths. With such a grid, minimal effect of the filter on the physical oscillations is ensured. Regarding the strategy of implementation, since the initially developed oscillations at the discontinuity are of 2Δ wavelength and the distribution of wavelength tends to widen with time, the filter is most effective when applied at each time step of the computation.

For the elliptic flow problem, the filter can substantially improve the performance of both central difference and QUICK schemes. For the 1D flow with a shock and a simple wave equation, the spurious oscillations can also be completely suppressed, resulting in highly satisfactory numerical solutions, even with a very simple computational procedure and a first-order-accurate scheme. In this regard, a relaxation procedure is proposed which is shown to be capable of further improving the solution qualities. The interaction of wavelength and filtering with relaxation is currently under study. The results presented so far contain only one shock or sharp gradient region. For more com-

plicated cases that involve the interaction of the waves of sharp gradients, the exact performance of the present filtering technique is not clear and needs to be further investigated.

Conventionally, to resolve sharp gradients numerical dissipation is usually employed to obtain a physically realizable solution, while compromising on accuracy. The present results demonstrate that the filter, when used with a higher order dispersive scheme, provides an interesting alternative, allowing the accuracy of the dispersive scheme to emerge, while maintaining physical realizability.

REFERENCES

1. P. J. Roache, *Computational Fluid Dynamics* (Hermosa, Albuquerque, NM, 1972).
2. C. Hirsch, *Numerical Computation of Internal and External Flows*, Vol. 2, (Wiley, New York, 1990), part VII.
3. P. Gresho and R. Lee, *Comput. Fluids* **9**, 223 (1981).
4. H. A. Dwyer, M. O. Smooke, and R. J. Kee, *AIAA J.* **18**, 1205 (1980).
5. P. R. Eiseman, *Comput. Methods Appl. Mech. Eng.* **64**, 321 (1987).
6. W. Shyy, *Int. J. Numer. Methods Fluids* **8**, 475 (1988).
7. M. Berger and A. Jameson, *AIAA J.* **23**, 561 (1985).
8. I. Babuska, O. C. Zienkiewicz, J. Gago, and E. R. Oliveira, (Eds.) *Accuracy Estimates and Adaptive Refinements in Finite Element Computations* (Wiley, New York, 1986).
9. D. G. Holmes and S. Conner, "Solution of the 2D Navier-Stokes Equations on Unstructured Adaptive Grids," AIAA 9th Computational Fluid Dynamics Conference, Buffalo, NY, June 13, Paper No. 89-1932, 1989 (unpublished).
10. B. Engquist, P. Lotstedt, and B. Sjogreen, *Math. Comput.* **52**, 509 (1989).
11. W. Shyy, *J. Comput. Phys.* **57**, 415 (1985).
12. B. P. Leonard, *Comput. Methods Appl. Mech. Eng.* **19**, 59 (1979).
13. D. A. Anderson, J. C. Tannehill, and R. H. Pletcher, *Computational Fluid Mechanics and Heat Transfer* (Hemisphere, New York, 1984).
14. S. Osher and S. Chakravarthy, *SIAM J. Numer. Anal.* **21**, 955 (1984).
15. J. L. Steger and R. F. Warming, *J. Comput. Phys.* **40**, 263 (1981).